Article

pubs.acs.org/Biomac

Intracellular Routing in Breast Cancer Cells of Streptavidin-Conjugated Trastuzumab Fab Fragments Linked to Biotinylated Doxorubicin-Functionalized Metal Chelating Polymers

Peng Liu,[†] Zhongli Cai,[‡] Jae W. Kang,[†] Amanda J. Boyle,[‡] Jarret Adams,[§] Yijie Lu,[†] Ghislaine Ngo Ndjock Mbong,[‡] Sachdev Sidhu,[§] Raymond M. Reilly,*[,‡,∥] and Mitchell A. Winnik*[,†]

[†]Department of Chemistry, University of Toronto, 80 St. George Street, Toronto, Ontario, Canada, M5S 3H6

[‡]Department of Pharmaceutical Sciences, University of Toronto, 144 College Street, Toronto, Ontario, Canada M5S 3M2

[∥]Toronto General Research Institute, University Health Network, Toronto, Ontario, Canada, M5G 2M9

[§]Terrence Donnelly Center for Cellular and Biomolecular Research, University of Toronto, 160 College Street, Toronto, Ontario, Canada M5S 3E1

Supporting Information

ABSTRACT: We describe the synthesis of a heterotelechelic metal-chelating polymer (Bi-MCP-Dox), a polyacrylamide with a number average degree of polymerization DP_n = 50 (PDI = 1.2), with biotin (Bi) and doxorubicin (Dox) as functional chain ends and diethylenetriaminepentaacetic acid (DTPA) pendant groups as the binding sites for metal ions. We compared its behavior in cell-uptake experiments with a similar polymer (Bi-MCP) without Dox. These MCPs were complexed with trastuzumab Fab (tmFab) fragments covalently linked to streptavidin (SAv) to form tmFab-SAv-Bi-MCP-Dox and tmFab-SAv-Bi-MCP via the strong affinity between Bi and SAv. tmFab targets human epidermal growth factor receptor-2 (HER2), which is overexpressed on certain human breast cancer cells. Surface plasmon resonance (SPR) experiments with the extracellular domain (ECD) of HER2 showed that incorporation of the MCPs in these complexes had no significant effect on the association or dissociation rate with the HER2 ECD and the dissociation constants. The tmFab-complexed MCPs were subsequently labeled with ^{111}In (an Auger electron emitting radionuclide). Auger electrons can cause lethal DNA double strand breaks (DSBs) but only if they are emitted intracellularly and especially, in close proximity to the nucleus. To evaluate the cellular and nuclear uptake of tmFab-SAv-Bi-MCP-Dox, we incubated HER2+ SK-BR-3 human breast cancer cells with the complexes saturated with stable In^{3+} and visualized their distribution by confocal fluorescence microscopy, monitoring the fluorescence of Dox. In parallel, we carried out cell fractionation studies on tmFab-SAv-Bi-MCP-Dox and on tmFab-SAv-Bi-MCP labeled with ^{111}In. Both radiolabeled complexes showed cell internalization and nuclear localization. We conclude that metal-chelating polymers with this composition appear to encourage internalization, nuclear uptake, and chromatin (DNA) binding of trastuzumab fragments modified with streptavidin in human breast cancer cells expressing HER2. Further study is needed to understand the impact of polymer charge on cellular uptake and distribution to intracellular compartments.

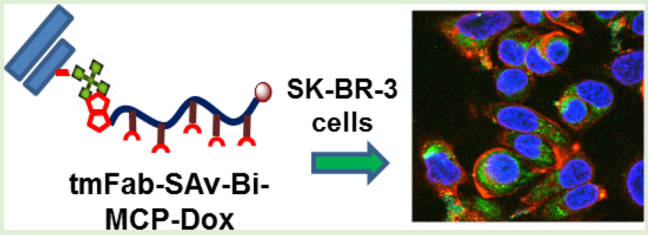

INTRODUCTION

HER2 is the second member of the human epidermal growth factor receptor (EGFR) family, and is encoded by the HER2/*neu* proto-oncogene.[1] Overexpression of HER2 is associated with a wide spectrum of cancers, including lung, breast, and ovarian, as well as adenocarcinomas of the colon and salivary gland.[2−4] In 1987, Slamon et al. reported that overexpression of HER2 was found in about 30% of 189 primary breast carcinomas and was correlated with a poor prognosis.[5] Moreover, overexpression of HER2 may contribute to the transformation of normal cells into a neoplastic phenotype.[6,7] Because of its ready accessibility as a transmembrane glycoprotein and the limited expression of HER2 in most normal cells except cardiac myocytes, numerous studies have focused on immunotherapy of HER2-positive tumors.[8]

For more than 20 years, the humanized monoclonal antibody trastuzumab (Herceptin) has been widely used for the treatment of HER2-positive metastatic breast cancer.[9] The mechanism of action of trastuzumab is not completely understood, but this agent combined with chemotherapy (e.g., paclitaxel or docetaxel) is now the standard-of-care for this type of breast cancer.[10] Nonetheless, only half of the patients with HER2-positive metastatic breast cancer benefit

Received: October 3, 2013
Revised: January 24, 2014
Published: February 7, 2014

from trastuzumab-chemotherapy combinations, and almost all patients who initially respond to this treatment acquire resistance within a year.[10]

Several strategies to increase the effectiveness of trastuzumab therapy for HER2-positive tumors have been reported. These approaches couple HER2 targeting using trastuzumab with the delivery of cytotoxic agents to tumor cells.[11−14] For example, trastuzumab has been chemically modified with an anthracycline[12] (which binds to DNA) and auristatin[13] (that disrupts microtubules) to improve the therapeutic index, or with mytansinoid (DM1), which also targets microtubules. The conjugate trastuzumab-DM1 has proven to be very effective for treatment of HER2-positive breast cancer, including tumors that have developed resistance to treatment with trastuzumab-containing regimens.[14]

Another emerging approach is to generate radioimmunoconjugates (RICs) by labeling trastuzumab with cytotoxic radionuclides. Costantini, et al.[15] derivatized trastuzumab with DTPA as a carrier of ^{111}Indium (^{111}In), which emits Auger electrons in addition to its γ-emissions. These electrons have low energy (<25 keV) and deposit this energy over nanometer-micrometer distances resulting in high linear energy transfer, which causes nuclear DNA double strand breaks. However, because of the ultrashort range of these electrons, ^{111}In is most effective for causing lethal DNA breaks if it is in close proximity to the cell nucleus. For this reason, Costantini et al. also derivatized trastuzumab with multiple copies of a nuclear-localizing sequence (NLS) peptide. The NLS peptides are believed to interact with importins α/β, which are intracellular transport proteins that enable translocation across the nuclear pore complex. These authors found that ^{111}In-NLS-trastuzumab was 8-fold more potent on a concentration basis at decreasing the clonogenic survival of HER2 amplified SK-BR-3 cells with high HER2 density (2×10^6 per cell) than unlabeled trastuzumab.

One limitation of ^{111}In-NLS-trastuzumab was its low specific activity (SA). In the example referred to above, the SA achieved indicated that only 1 in 50 antibodies were labeled with ^{111}In.[15] Thus, in the clonogenic assay experiments, a large proportion of the targeted HER2 was bound by nonradiolabeled antibodies. This problem can in principle be overcome by attaching a metal chelating polymer (MCP)[16] with multiple sites for complexing ^{111}In to trastuzumab. In this way, the probability that each antibody carried one or more radionuclides would be substantially enhanced.

Recently we described a facile approach to append MCPs, each carrying multiple diethylenetriaminepentaacetic acid (DTPA) groups for complexing ^{111}In, onto Fab fragments of trastuzumab (tmFab) with the idea of amplifying the radiometal ion delivery per HER2 recognition event.[17−19] tmFab was first linked covalently to streptavidin (SAv) through a polyethylene glycol (PEG_{24}) spacer. A series of biotinylated MCPs (Bi-MCP), each bearing a terminal biotin, was synthesized for noncovalent but high affinity ($K_a = 10^{15}$ M^{-1}) binding to the SAv moiety. Our goal was to examine a family of MCPs that differed in backbone structure (polyacrylamide, polypeptide), chain length, and pendant groups, with the goal of exploring how these factors affected biodistribution in vivo and cell uptake in vitro.

These polymers were synthesized by "living" polymerization reactions that allowed control over chain length and end group functionality and yielded polymers with narrow length distributions. Because of the terminal biotin group, these polymers could be rapidly bound to tmFab-SAv and then labeled with ^{111}In. One type of polymer, with a polyacrylamide backbone, was synthesized by reversible addition−fragmentation transfer (RAFT) polymerization.[18] Polypeptide polymers with a polyaspartamide backbone or a polyglutamide backbone were synthesized by ring-opening polymerization of the corresponding benzylaspartate *N*-carboxyanhydride (NCA) and benzylglutamate NCA.[19] Following construction and characterization of the polymer backbone, the DTPA groups were introduced by a sequence of pendant group transformations that maintained the overall length of the polymer. In this way, polymers with a number average degree of polymerization (DP_n) of 20 to 50 monomer units per polymer were obtained, with polydispersities (PDI) in the range of 1.1 to 1.2.

In a recent study, we examined the influence of MCP structure on the tumor and normal tissue biodistribution of trastuzumab in a mouse model, particularly the effects of the charge and backbone composition of the polymers. These experiments involved Bi-MCPs with polyacrylamide [Bi-PAAm($DTPA_{40}$)] and polyglutamide [Bi-PGlu($DTPA_{28}$)] or polyaspartamide [Bi-PAsp$(DTPA)_{33}$] backbones linked to SAv-tmFab and labeled with ^{111}In.[17] The effect of saturation of uncomplexed DTPA groups with stable In^{3+} ions was also examined. Biodistribution was assessed by microSPECT/CT imaging and by ex vivo γ-scintillation counting of tissues by taking advantage of the two γ-photons emitted by ^{111}In. Our results showed that MCPs with a zwitterionic polyglutamide backbone were the most suitable for constructing polymer-tmFab immunoconjugates, since these exhibited the lowest accumulation in the liver and preserved the specific tumor accumulation of tmFab in HER2-overexpressing SKOV-3 human ovarian cancer xenografts in athymic mice.[17] High liver uptake was observed for MCPs with a polyacrylamide backbone, an effect that we attributed to the negative charges associated with the repeat unit of this polymer. Saturating uncomplexed DTPA groups with In^{3+}lowered the net charge per repeat unit of the polymer and decreased the liver uptake of the RIC. The maximum specific activity for labeling with ^{111}In was increased by more than 100-fold for the MCPs compared to tmFab conjugated to two DTPA per molecule.[18]

In this paper we describe cell uptake experiments with HER2-overexpressing SK-BR-3 cells with a pair of tmFab-SAv-Bi-MCP complexes in which we compared two carefully matched MCPs. One was a novel heterotelechelic polyacrylamide MCP that contained a biotin group at the initiating end to permit linkage to tmFab-SAv, and a covalently bound doxorubicin (Dox) at the other end. The other was biotin-polyacrylamide of very similar length and composition, lacking the terminal Dox. Both were synthesized by RAFT polymerization. Doxorubicin is a widely used anticancer drug.[20] Dox interacts with proteosomes and is subsequently transferred to the cell nucleus, where it intercalates into DNA, inhibiting DNA replication, leading to apoptosis.[20] Dox has been found to be a radiosensitizer for the DNA-damaging effects of the Auger electrons emitted by ^{111}In, possibly by inhibiting DNA repair.[21] In addition, a related analog, daunorubicin labeled with the Auger electron-emitter ^{125}I, has been shown to directly cause DNA strand breaks in SK-BR-3 cells.[22]

In this study, we hypothesized that Dox could act as a nuclear localization moiety for MCPs to deliver ^{111}In into close proximity to DNA to maximize its lethal DNA-damaging effects. From a practical point of view, Dox has an optical

Scheme 1. Synthesis Route for Bi-DTPA and Dox-Maleimide (A) and for Biotin Containing RAFT Polymer (B)

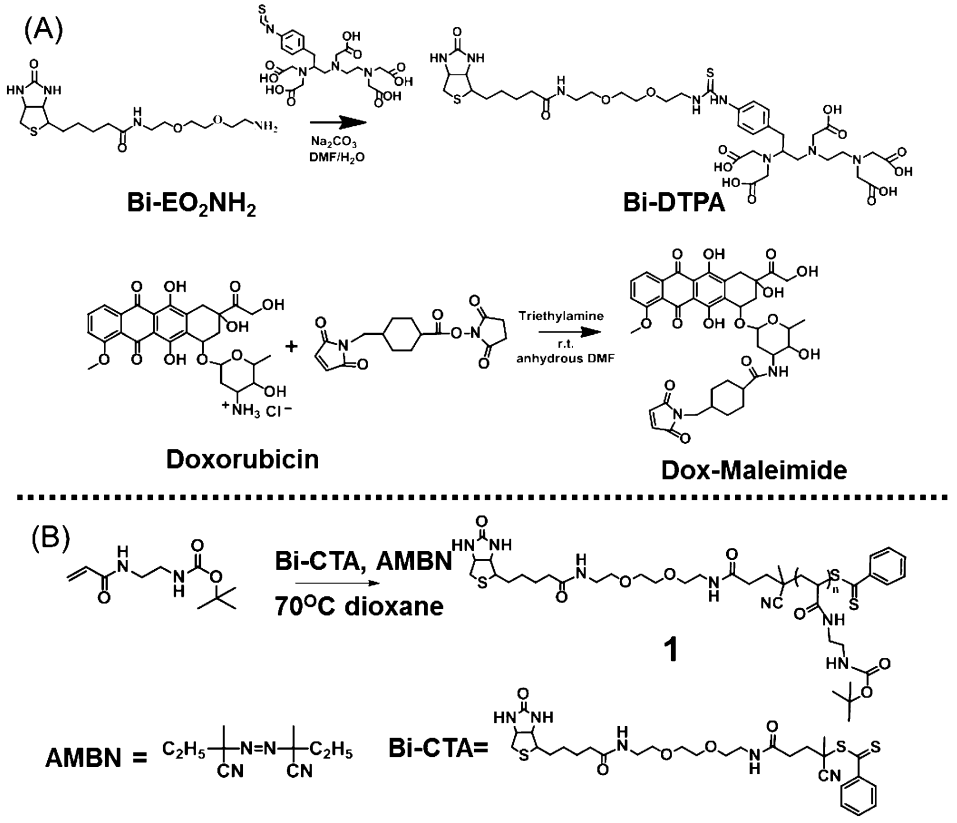

Scheme 2. Synthesis Route for Bi-PAAm(DTPA)$_{50}$-Dox and the Chemical Structure of Bi-PAAm(DTPA)$_{50}$[a]

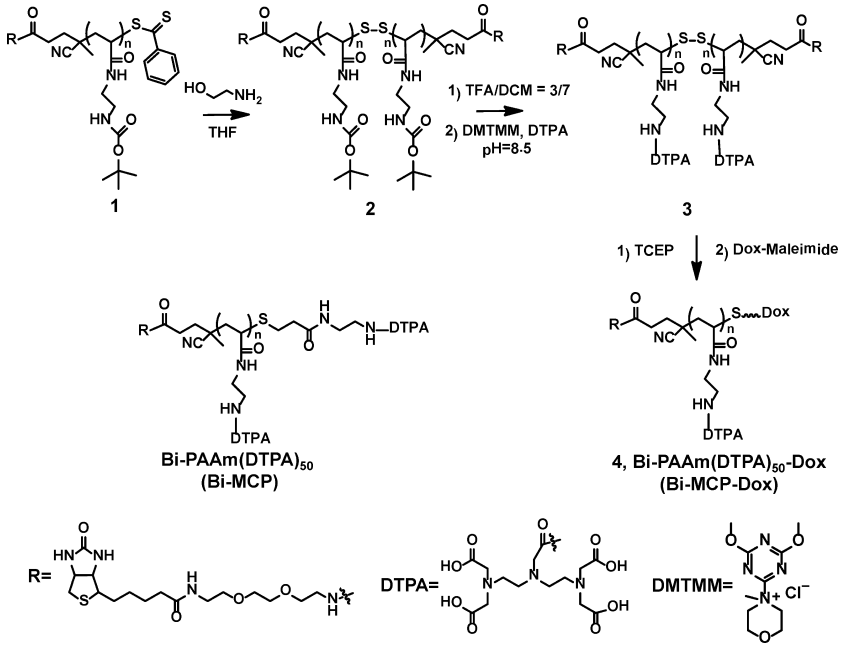

[a]These two polymers have the same backbone structure and biotin end groups, as well as almost identical chain lengths.

absorption band in the visible region of the spectrum (λ_{ab} = 480 nm), and its strong characteristic fluorescence (λ_{em} = 550 nm) enables visualization of its intracellular distribution by confocal microscopy. In cell fractionation studies, we compared the behavior of tmFab-SAv-Bi-MCP-Dox with tmFab-SAv-Bi-MCP, the essentially identical MCP lacking the Dox end group. In these experiments, tmFab-SAvs were complexed with MCPs that were labeled with ^{111}In. Their intracellular routing was determined by measuring the radioactivities of isolated cell compartments. In addition, we used surface plasmon resonance (SPR) measurements employing the extracellular domain (ECD) of HER2 to determine the effect of linking of Bi-

dx.doi.org/10.1021/bm401483a | Biomacromolecules 2014, 15, 715−725

MCP and Bi-MCP-Dox to tmFab-SAv on the binding affinity of the Fab fragments.

Our most important result was that the MCP itself strongly promoted cell uptake and delivery to the cell nucleus. The polymer with the terminal Dox led to somewhat lower nuclear uptake. These findings have important implications for the future development of MCPs as carriers of ^{111}In in radioimmunoconjugates intended for Auger electron radioimmunotherapy.

EXPERIMENTAL SECTION

Instrumentation. *HPLC and SEC.* Size exclusion chromatography (SEC) measurements of precursor polymers were conducted with *N*-methylpyrrolidone (NMP) containing 0.2 wt % LiCl as the eluent at 80 °C. Water-soluble MCPs were examined by aqueous SEC with an eluent of phosphate buffer (pH 8.5, 25 mM, containing 0.2 M KNO_3 and 200 ppm NaN_3). High pressure liquid chromatography (HPLC) measurements of samples containing tmFab or ^{111}In were conducted using 100 mM NaH_2PO_4 buffer, pH 7.0, as eluent. Measurements of small organic molecules were conducted by HPLC with mass spectrometry detection (HPLC-MS) using a C18 column. The gradient consisted of eluents A (water with 1% formic acid) and B (acetonitrile with 1% formic acid). Details are provided in the Supporting Information (SI).

Other Instrumentation. ^{1}H NMR measurements employed a Varian 400 spectrometer operating at 400 MHz. The γ-counter used for radioactivity measurements was a 1480 Wizard 3 (Perkin Elmer, Turku, Finland). ESI mass analyses were performed on QStar model quadrupole time-of-flight mass spectrometer (AB Sciex, Concord, ON). MALDI-TOF spectra were obtained on Waters MICROMASS MALDI micro MX Mass Spectrometer. The reflectron mode was employed for measurements of doxorubicin-maleimide (Dox-Maleimide) with dithranol as the matrix. Confocal fluorescence images were obtained with a Zeiss LSM 510 confocal microscope with a Plan-Apochromat 6.3×/1.2 water objective and laser scanning set to z-stack mode. The fluorescence excitation laser wavelengths were set to 555, 405, and 488 nm, respectively, to excite three different dyes. Surface plasmon resonance (SPR) measurements were performed on a ProteOn XPR36 Protein Interaction Array System (BioRad).

Materials. The biotin-end-capped metal chelating polymer Biotin-poly(3,6,9-triscarboxymethyl-3,6,9-triazaundecandioicacid-amido-*N*-ethylamido acrylamide) [Bi-PAAm(DTPA)$_{50}$], with a mean degree of polymerization of $DP_n \approx 50$, was previously reported in ref 18. For simplicity, this MCP is referred to as "Bi-MCP". The synthesis and characterization of 3,6,9-triscarboxymethyl-3,6,9-triazaundecandioica-cid-amido-3,6-dioxaoctane-1,8-biotinamide (Monobiotin-DTPA, Bi-DTPA) as well as doxorubicin-maleimide (Dox-Maleimide; see Scheme 1) are described in the SI.

Synthesis of a Heterotelechelic MCP with a Terminal Doxorubicin. Polymer synthesis began with the RAFT polymerization of N-{2-[(BOC) aminoethyl]} acrylamide (BocNAAm) with a biotin-containing chain transfer agent as described in ref 18. Through a series of postpolymerization modifications, the dimeric polymer Bi-PAAm(DTPA)$_{50}$-disulfide (polymer **4**, Scheme 2) was synthesized and served as a precursor to attach a terminal Dox. The details of the synthesis and characterization are given in the SI.

Reduction of the Disulfide and Attachment of Dox to the Polymer. A solution of TCEP (0.5 M) was freshly prepared in HEPES buffer (20 mM). Bi-PAAm(DTPA)$_{50}$-disulfide (10 mg) was dissolved in HEPES buffer (2 mL). An aliquot of the TCEP solution (0.1 mL) was added, and the mixture was stirred for 4 h at 40 °C. Dox-maleimide (1.51 mg, 1.98 mmol) was dissolved in DMF (8 mL); this solution was added to the TCEP-treated MCP solution, and the mixture was stirred overnight at 40 °C. The solution was diluted with ethanol/water (1:1 v/v, 13 mL), transferred to a 15 mL 3kDA MWCO Millipore Amicon spin filter, and washed with the ethanol/water mixture (5 × 11 mL), followed by DI water (5 × 11 mL). Finally, the aqueous solution was freeze-dried to yield the Dox-end-labeled DTPA polymer (9.2 mg) (Bi-PAAm(DTPA)$_{50}$Dox, which we will also refer to as "Bi-MCP-Dox".

Breast Cancer Cells. HER2+ SK-BR-3 cells were purchased from the American Type Culture Collection (Manassas, VA, U.S.A.) and cultured in RPMI 1640 medium (Sigma-Aldrich, St Louis, MO, U.S.A.) supplemented with 10% fetal bovine serum (FBS, Gibco-Invitrogen Inc., Carlsbad, CA, U.S.A.) and 1% penicillin-streptomycin (P/S, Gibco-Invitrogen Inc.). A nuclei isolation kit (Nuclei EZ Prep Nuclei Isolation Kit, NUC-101; Sigma-Aldrich) was used to separate the cell nuclei from the cytoplasm. The 6-well cell plates were purchased from Sarstedt. In the cell staining experiments we used Hoechst 33342 dye (Molecular Probes, Inc.) to stain cell nuclei and wheat germ agglutinin-Alexa Fluor 594 (WGA-Alexa) to stain cell membranes (Molecular Probes, Inc.). The buffers for the In^{3+} labeling were treated with Chelex-100 resin (Biorad) to remove cationic trace metals.

Preparation of Immunoconjugates Containing tmFab-SAv. Fab fragments of trastuzumab (tmFab) and streptavidin-conjugated tmFab (tmFab-SAv) were prepared as reported by Boyle et al.[17] To form complexes of tmFab-SAv with biotin-functionalized MCPs and with Bi-DTPA, solutions of the two components were prepared in PBS at 1 mg/mL. The conjugate was prepared by mixing tmFab-SAv with Bi-MCPs in a 1:1 mol ratio and stirring for 1 h at room temperature. tmFab-SAv and Bi-DTPA were mixed in a mole ratio of 1:3.

Preparation of Immunoconjugates for Confocal Fluorescence Microscopy. PBS containing $InCl_3$ (stable indium) solution in sodium acetate (NaOAc) buffer (100 mM, pH 6.0, 8.6 μL) was added to the tmFab-SAv-Bi-MCP-Dox (11 μg polymer and 37 μg tmFab-SAv) in PBS prepared as described above. The mixture was kept at room temperature for 1 h. In order to remove excess In^{3+}, the solution was subsequently transferred to a 30 kDa MWCO spin-filter, diluted with NaOAc buffer and washed with several passages of NaOAc buffers (10 × 400 μL, pH 6.0, 100 mM). The residual solution in the upper chamber of the spin-filter was then diluted with PBS buffer (3 mL, pH 7.4) and collected.

Preparation of RICs for Cell Fractionation Studies. Two cell fractionation experiments were conducted. In the first experiment, tmFab-SAv (7.5 μg) complexed with Bi-MCP (2.2 μg), Bi-MCP-Dox (2.2 μg), Bi-DTPA (0.2 μg) were compared. The RICs were radiolabeled with $^{111}InCl_3$ in NaOAc buffer (pH 6.0) to a specific activity of 0.25 MBq/μg at RT for 1 h. In the second experiment, two samples of tmFab-SAv-Bi-MCP–^{111}In were prepared. One was used directly. The other RIC was treated for 1 h with an excess of stable $InCl_3$ solution (3.39 μL, 3 mg/mL) to saturate the In^{3+} binding sites on the polymers. The RICs were purified from free In^{3+} by spin-filter tubes (50 kDa MWCO). The labeling efficiency of the three samples was measured by instant thin layer silica gel chromatography (ITLC-SG) developed in 100 mM sodium citrate, pH 5.0. The labeling efficiency of tmFab-SAv-Bi-MCP-Dox was 99.6% and that of tmFab-SAv-Bi-MCP was 99.5%. The labeling efficiency of tmFab-SAv-Bi-DTPA was 79%. After one-time purification by spin-filter (50 kDa MWCO, $1.5 \times 10^4 \times$ g, 10 min), its radiochemical purity increased to 97%.

Surface Plasmon Resonance (SPR) Measurements. The ECD of HER2 (R&D Systems, Minnesota, U.S.A.) in 50 mM phosphate buffer (pH 4.5) was immobilized onto an EDAC/sulfo-NHS activated sensor chip surface at 30 μL/min for 5 min in the vertical direction. Immobilization levels were monitored to ensure approximately 500 response units were immobilized; a second injection was used if needed. Immobilized ECDs were then stabilized with PBS for 30 s and 0.85% H_3PO_4 for 18 s, each at 100 μL/min. For the Fab binding assays, the highest concentration used for tmFab-SAv was 246 nM, and this solution was further diluted with PBS containing 0.05% Tween 20 in 2-fold series to produce a series of five concentrations ranging from 246 to 15.4 nM. Binding measurements of tmFab-SAv-Bi-MCP and tmFab-SAv-Bi-MCP-Dox were initiated with a concentration of 122 nM, followed by serial dilution to obtain five concentrations ranging from 122 to 7.6 nM. All the binding assays were carried out at 25 °C at a flow rate of 100 μL/min for 1 min. The dissociation steps were monitored for 10 min. The kinetic parameters were calculated by

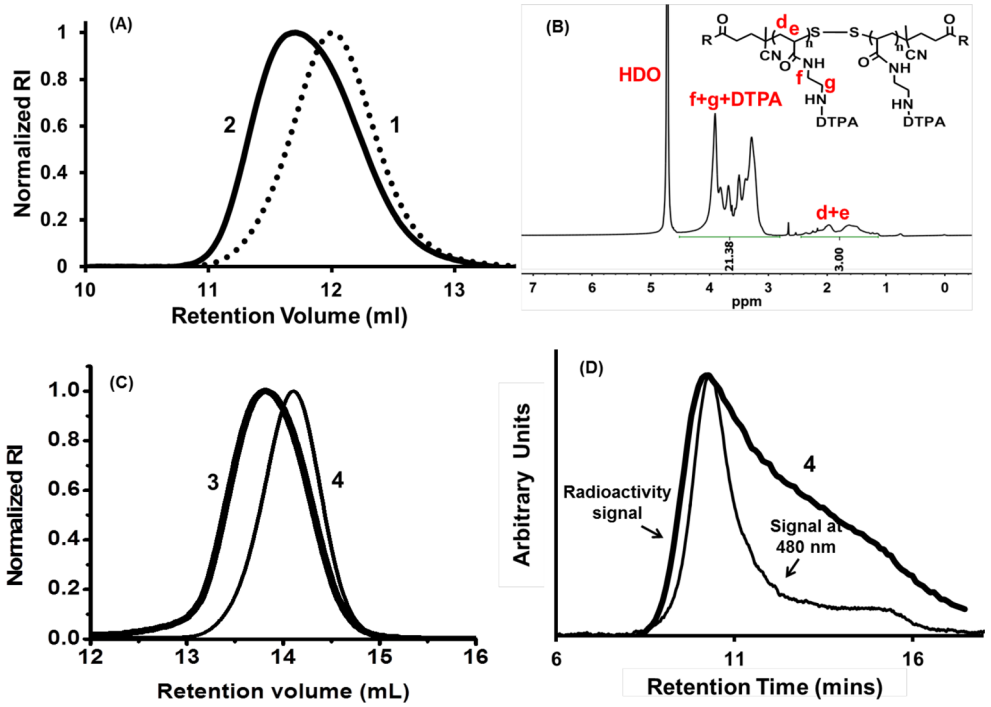

Figure 1. (A) Comparison of SEC chromatograms in NMP (with 0.2 wt % LiCl) at 80 °C of the RAFT polymer **1** (dashed line) and polymeric dimer **2** (solid line) formed through the disulfide bond linkage. The chromatogram demonstrates the earlier elution time of the polymeric dimer in comparison with the RAFT polymer due to its larger molecular weight. The traces were analyzed by comparing with PMAA standards. (B) ^{1}H NMR of Bi-PAAm(DTPA)$_{51}$-disulfide **3**. The integration of peaks from the polymer shows that about 97% of the pendant groups were functionalized with DTPA. (C) Comparison of SEC traces of Bi-MCP-disulfide **3** and the polymer after TCEP reduction **4** in water at 30 °C containing 0.2 M KNO_3, 25 mM phosphate buffer (pH 8.5), and 200 ppm NaN_3. The traces were analyzed by comparison to PMAA standards. The thicker line refers to the disulfide polymer and the thinner line represents the polymers after TCEP reduction. The retention volume shift and the narrower polydispersity of the TCEP-treated polymer imply the reduction of the disulfide bond. (D) HPLC chromatogram (BioSep-SEC-4000 column, 300 × 4.6 mm) of radiolabeled Bi-MCP-Dox monitored at 480 nm and with a radioactivity detector. The eluent was 0.1 M NaH_2PO_4 at pH 7.0 at a flow rate of 0.35 mL/min. The MCP (0.5 μg/μL in PBS buffer) was labeled with ^{111}In (2 MBq) and 20 μL was injected; UV−vis detector was set at 480 nm. The broader peak from the radioactivity signal is due to the larger flow cell for this detector.

ProteOn manager software (Bio-Rad Laboratories Ltd. Hercules, CA, U.S.A.). Analysis was conducted using the kinetic Langmuir model.[23]

Confocal Fluorescence Microscopy. SK-BR-3 cells in RPMI 1640 medium supplemented with 10% FBS were seeded on coverslips (12 mm diameter) in 24-well plates. Three groups of experiments were conducted. In the first, the cells were cocultured with tmFab-SAv-Bi-MCP-Dox. Before adding the immunoconjugates to the cells, the concentration of Dox in the solutions was measured by UV−vis at 480 nm. In the second group, cells were cocultured with free Dox at the same concentration of Dox as the first group. In the third group of experiments, the cells were treated for 10 min with a 100-fold excess of trastuzumab compared to the tmFab-SAv-Bi-MCP-Dox complex to saturate HER2 receptors on the cell surface and then cocultured with tmFab-SAv-Bi-MCP-Dox to study the nonspecific adsorption of tmFab-SAv-Bi-MCP-Dox to the cells. All experiments were performed in triplicate. After incubation at 37 °C overnight, the cells were rinsed with PBS and incubated with Hank's Balanced Salt Solution (HBSS) containing WGA-Alexafluor immunoconjugates (1 μg/mL) and Hoechst 333324 (4 μg/mL) at 37 °C for 10 min to stain the cell membranes and nuclei, respectively, and then fixed with 2% paraformaldehyde PBS solution. Accumulation of the tmFab-SAv-Bi-MCP-Dox complex within the cells, based on Dox fluorescence, was observed by confocal fluorescence microscopy in the *z*-stack mode with Dox excitation at 488 nm, and detection in the range 490 to 537 nm. Fluorescence excitation for Alexa Fluor 594 was 555 nm with emission detected at 569 to 679 nm, and for Hoechst 333324, excitation was 405 nm, with emission detected at 400 to 550 nm.

Cell Fractionation Studies. Subconfluent SK-BR-3 cells were harvested by trypsinization and seeded into 6-well tissue culture plates (5×10^5 cells and 1 mL medium per well). The cells were then cultured for 24 h. After culturing overnight, the cells were treated with RICs (tmFab-SAv-Bi-MCP−^{111}In, tmFab-SAv-Bi-MCP-Dox-^{111}In and tmFab-SAv-Bi-DTPA-^{111}In) for another 16 h in the presence of serum-free medium. The concentration of Fab in each well was 10 nM. After incubating the cells with RICs for 16 h, the cells were first rinsed with PBS to remove unbound RICs. Then the cells attached to the plates were treated with 200 mM NaOAc in 500 mM NaCl, pH 2.5 to remove cell surface-bound radioactivity, followed by rinsing with PBS. Both the acidic solution and the rinsing PBS solution were collected and counted in a gamma counter. Immediately after, cell lysis buffer was added into the wells, and the cell culture plates were put on ice for 40 min. Cell scrapers were then employed to transfer the lysed cells into centrifuge tubes. After centrifugation, the supernatant was collected, and the radioactivity in this fraction representing internalized RICs in the cytoplasm was counted in a γ-counter. The nuclear pellet was then sequentially treated with buffers consisting of (i) 0.2 M sucrose/3 mM $CaCl_2$/ 50 mM Tris Cl, pH 7.6, (ii) 0.14 M NaCl/10 mM Tris Cl, pH 8.3, and (iii) 1 mM Tris Cl, pH 7.9. Cell nuclei and chromatin (DNA) were isolated from cells following the method reported by Reilly et al.[24] After each buffer treatment, the solutions were centrifuged, and the supernatants were collected and combined. Chromatin was collected as the pellet after the last centrifugation cycle.

In the second group, cell fractionation experiments with tmFab-SAv-Bi-MCP−^{111}In were compared with experiments that employed tmFab-SAv-Bi-MCP−^{111}In saturated with excess stable In^{3+}. Cells were cultured and treated with RICs in the same manner described above. Experiments for both groups, In^{3+}-saturated RICs and the RICs without stable In^{3+}, were conducted in triplicate. In these experiments the nuclear radioactivity was measured without further fractionation.

dx.doi.org/10.1021/bm401483a | *Biomacromolecules* 2014, 15, 715−725

RESULTS AND DISCUSSION

Synthesis of the Biotinylated MCP with a Terminal Dox. MCPs with a biotin at one end were synthesized by RAFT polymerization of N-{2-[(BOC) aminoethyl]} acrylamide (BocNAAm), as previously described,[18] using a biotin-containing chain transfer agent (Scheme 1B). Following the approach described by Majonis et al.,[25] the RAFT end group was removed by aminolysis, and then the terminal thiol groups were oxidized to yield dimeric disulfide-coupled polymers. The disulfide groups protect the terminal thiol groups during pendant group modification of the polymer. Due to the sensitivity of Dox to the reaction conditions employed for pendant group transformation of the initially prepared RAFT polymer, the strategy was designed to allow for attachment of Dox to the chain terminus in the last step of the synthesis. The disulfide bonds of the MCPs were reduced to thiols with TCEP, followed by reaction with a Dox derivative containing a maleimide substituent.

The mean degree of polymerization (DP_n) of the Bi-PBocNAAm polymer was characterized by ^{1}H NMR end group analysis (Figure S1), comparing the integration of the peaks of the dithiobenzoate protons at 7.91, 7.57, and 7.39 ppm to the integral of signals of the peaks ranging from 2.59 to 0.38 due to the polymer backbone protons and the *tert*-butyl groups. For this polymer we obtained DP_n = 50. Based on previous experience with this type of polymer,[18,25] we assumed that DP_n did not change significantly during the pendant group transformations.

Pendant Group Modification. In order to preserve functionality at the polymer terminus during pendant group modification and introduction of the DTPA metal chelating groups, the dithiobenzoate group from the RAFT polymerization was removed by aminolysis with excess ethanolamine in THF (Scheme 2). The reaction was carried out in air to promote oxidation of the thiol end groups to a disulfide, which serves to protect the thiols during subsequent reactions of the pendant groups. In the SEC chromatogram (Figure 1A), the RAFT polymer after aminolysis and oxidation (dashed line) shows a broader peak and an earlier elution time than the precursor polymer (solid line). The dimeric disulfide-bridged polymer was then treated with TFA in DCM to remove the tBoc groups. The reaction was essentially quantitative. The product polymer in the form of a polytrifluoroacetate salt was recovered by precipitation in diethyl ether. Introduction of DTPA groups followed a two-step protocol that we have previously reported.[18,25] In the first step, a large excess of DTPA was activated with a limiting amount of DMTMM (Scheme 2). Then a solution of the polymer in water was added, keeping the pH at 8.5. Excess DTPA and other small molecule byproducts were removed from the polymer by spin-filtration. The ^{1}H NMR spectrum of this polymer is presented in Figure 1B.

In the final step of the synthesis, the disulfides bridging the dimeric MCPs were reduced with TCEP to thiols. An aliquot was taken for analysis by SEC, and then Dox-Maleimide was added in situ. We chose TCEP as the reducing agent because the thiol addition to Dox-maleimide could be carried out without first purifying the polymer to remove excess reducing agent. The TCEP treated MCP showed a narrower peak and longer retention time than the disulfide-bridged MCP (Figure 1C). An aliquot of the final heterotelechelic MCP was then labeled with ^{111}In and characterized by SEC-HPLC equipped with both radioactivity and UV−vis detectors (Figure 1D). The overlap of the UV and radioactivity peaks indicates that the polymer contained both metal-chelating groups (DTPA) and Dox.

The Bi-PAAm$(DTPA)_{50}$Dox polymer (in the fully protonated state) has M_n = 23 kDa. In buffer solutions near neutral pH, the carboxylic acid groups of the polymers are partially dissociated. Previous experiments in our laboratory used thermal gravimetric analysis to characterize the state of dissociation of the carboxyl groups of a very similar MCP with pendant DTPA groups.[25] For this sample, neutralized at pH 8.5, washed extensively with DI water and then dried, there were on average about 2.2 Na^+ ions for each DTPA repeat unit. This number varies with pH and also with the extent of indium binding.

Complexation of MCPs with tmFab-SAv. Trastuzumab Fab fragments (tmFab) were covalently linked to streptavidin (SAv) with a poly(ethylene glycol) (PEG_{24}) spacer (tmFab-SAv) as described in ref 18. To complex MCPs to tmFab-SAv, the polymer and protein complex in a 1:1 molar ratio were incubated in PBS at pH 7.4 at RT for 1 h. An SEC-HPLC chromatogram of the complex is shown in Figure S8. In the SPR experiments described below, as well as in the confocal fluorescence microscopy and cell fractionation studies, the tmFab-SAv-Bi-MCP complexes were all prepared in the same manner.

HER2 Recognition. Our design of the RICs is based on the hypothesis that the Fab fragment of trastuzumab will retain its targeting ability toward HER2 after complexation with MCPs. In a previous publication,[18] we described cell binding experiments that evaluated the interaction of several tmFab-SAv-Bi-MCP-^{111}In complexes with SKOV-3 human ovarian cancer cells that overexpress HER2. One of the MCPs in those experiments was the Bi-PAAm $(DTPA)_{50}$ polymer employed here. In those experiments we compared radioactivity bound by cells exposed to the Fab immunoconjugates to that for cells coincubated with an excess of trastuzumab to determine the relative proportion of total and nonspecific binding, and by subtraction, the proportion of specific binding. Those experiments showed high specific binding (88.8 ± 2.1%) and low nonspecific binding for tmFab-SAv-DTPA-^{111}In, but only about 50% specific binding for tmFab-SAv-MCP-^{111}In. We concluded that RICs with MCPs can target HER2 on the surface of SKOV-3 cells but that nonspecific interactions occur.

In order to understand the binding affinity of the tmFab-SAv-Bi-MCP complexes for HER2, we employed surface plasmon resonance (SPR) measurements with the extracellular domain (ECD) of HER2 covalently immobilized onto a gold sensor chip. The association and dissociation rates were determined by modeling the increase and decrease in SPR signals in the sensorgrams (Figure 2). From the on-rates and off-rates, the association (k_a) and dissociation (k_d) rate constants were calculated. Association rate constants for tmFab-SAv-Bi-MCP and tmFab-SAv-Bi-MCP-Dox were similar to that of tmFab-SAv, and these values ranged from 1.2×10^5 to 1.9×10^5 M^{-1} s^{-1}. The dissociation rate constants were also similar in magnitude, ranging from 1.7×10^{-4} to 1.9×10^{-4} s^{-1}. From the ratio $k_d/k_a = K_d$, we determined that the dissociation constants for HER2 binding were in the low nanomolar range (Table 1). Based on the results of these experiments, we conclude that neither the polymer nor the terminal Dox group had a significant effect on the association rate, the dissociation rate, or the dissociation constant for the binding of SAv-tmFab

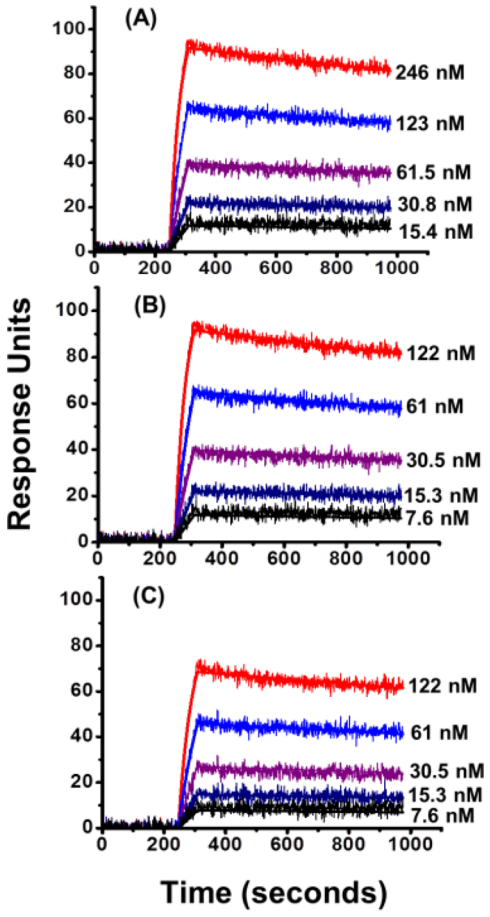

Figure 2. SPR plots of the binding and dissociation of tmFab-SAv complexes to an SPR gold chip coated with the ECD of HER2: (A) tmFab-SAv; (B) tmFab-SAv-Bi-MCP-Dox; (C) tmFab-SAv-Bi-MCP. In all three groups, five different concentrations were employed for the measurements, prepared by serially diluting the highest concentration by 2-fold. The order of experiments was from lowest concentration to highest. The highest concentration was 246 nM in (A) and 122 nM for both (B) and (C).

Table 1. Binding Kinetics Data from SPR Experiments at 25 °C

analyte	$10^{-5} \times k_a$[a] (M^{-1} s^{-1})	$10^{4} \times k_d$[b] (s^{-1})	K_D[c] (nM)	R_{max}[d]
tmFab-SAv	1.17 ± 0.01	1.79 ± 0.03	1.53 ± 0.03	109.96
tmFab-SAv-Bi-MCP-Dox	1.49 ± 0.01	1.92 ± 0.06	1.29 ± 0.04	82.24
tmFab-SAv-Bi-MCP	1.88 ± 0.01	1.65 ± 0.04	0.88 ± 0.03	90.67

[a]Values of the second order rate constant for the on-rate. [b]Values of the first order dissociation rate constant. [c]Values of the dissociation equilibrium constant. [d]Maximum response value.

immunoconjugates to the ECD of HER2. Although the absolute values for parameters describing the binding of SAv-tmFab immunoconjugates to the ECD of HER2 immobilized on gold chips is not directly comparable to those for binding to HER2 on cell membranes, the study within this SPR series allows us to compare the relative binding of the different complexes.[26]

Trastuzumab has been reported to bind to the ECD of HER2 with dissociation constant values K_d ranging from nanomolar to subnanomolar.[27,28] While it is difficult to compare binding constants for intact antibodies with those of Fab fragments because the intact antibody exhibits bivalent binding whereas Fab fragments are monovalent, it is interesting to note that the Fab complexes we examined have binding constants not substantially different from trastuzumab IgG. Previously, it was reported that the K_d values of trastuzumab and its Fab fragment were similar for binding HER2 in cell binding assays.[29] Thus, we conclude that tmFab-SAv-Bi-MCP complexes have sufficiently strong antigen recognition to deliver these RICs to cancer cells that overexpress HER2.

Intracellular Localization of Immunoconjugates. *Confocal Fluorescence Microscopy.* Exploiting the intrinsic fluorescence of Dox, we examined the cellular uptake and intracellular distribution of tmFab-SAv-Bi-MCP-Dox by confocal fluorescence microscopy. Images are shown in Figure 3.

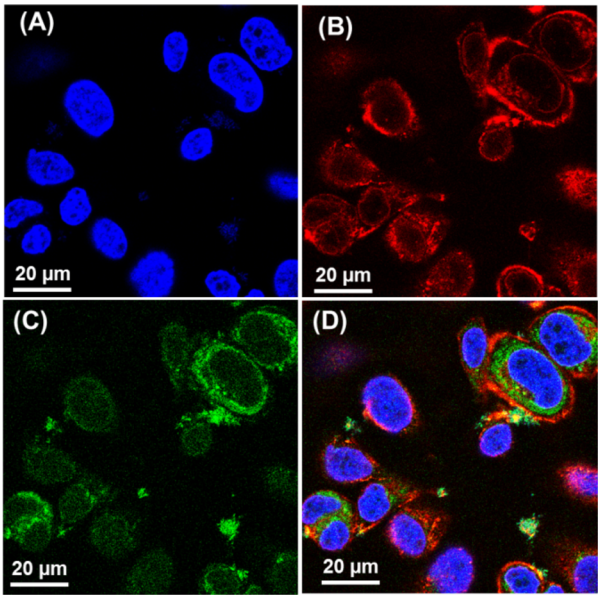

Figure 3. Individual and merged confocal fluorescence microscopy images of SK-BR-3 cells after incubating with tmFab-SAv-Bi-MCP-Dox overnight and counterstaining: (A) The cell nuclei stained with Hoechst 33342; (B) The cell membranes stained with WGA-Alexa immunoconjugates; (C) Dox fluorescence; (D) The merged fluorophore images.

The blue channel (Figure 3A) shows the cell nuclei (counterstained with Hoechst 33342), the red channel (Figure 3B) shows the cell membranes [stained with wheat germ agglutinin-Alexa Fluor 594 (WGA-Alexa)], and the green channel (Figure 3C) shows the location of the Dox-containing complexes. Figure 3D shows a superposition of all three fluorophores. From this image, one can tell that Dox fluorescence is localized inside the cell, close to the inner surface of the cell membrane. Dox fluorescence was found mainly in the cytoplasm and not in the cell nucleus. The Dox containing complexes exhibited punctate fluorescence, which may indicate endosome entrapment.[30] This type of staining is consistent with receptor-mediated endocytosis, which is likely due to the tmFab-HER2 interaction.[31]

The observation of cell internalization of tmFab is surprising, because it is well-known that endocytosis of Fab fragments is less efficient than endocytosis of intact antibodies.[31] This difference is thought to be related to the promotion of HER2 receptor clustering due to bivalent binding of intact antibodies,

dx.doi.org/10.1021/bm401483a | Biomacromolecules 2014, 15, 715−725

which is a requirement for the subsequent internalization. In Figure 3, the observation of extensive cell internalization of the tmFab-SAv-Bi-MCP-Dox complexes may be due to the properties of the MCP which encourage cellular penetration.

In Figure 4 we compare confocal fluorescence microscopy images of the tmFab-SAv-Bi-MCP-Dox-exposed cells with

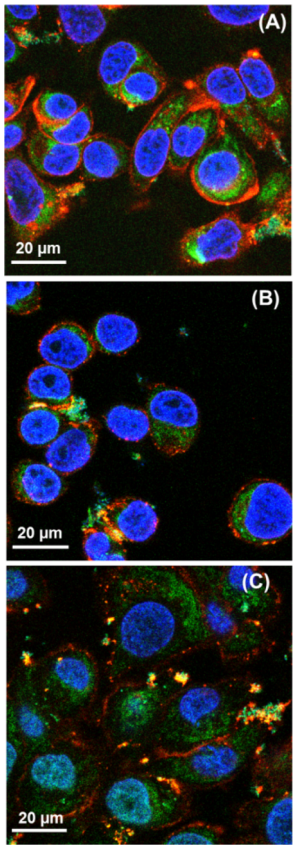

Figure 4. Images of SK-BR-3 cells incubated with tmFab-SAv-Bi-MCP-Dox (A) without pretreatment with trastuzumab and (B) after presaturation of HER2 with 100-fold excess of trastuzumab. Dox fluorescence is shown in green, whereas the cell membrane is stained red and the nucleus is stained blue (C) an image of the SK-BR-3 cells incubated with free Dox showing more diffuse cytoplasmic staining as well as nuclear uptake.

images obtained from two control experiments. The concentration of Dox in these experiments was monitored by UV−vis absorption at 480 nm to ensure that the same amount of Dox was used in each case. Figure 4A provides a second image similar to that shown in Figure 3D for the combined fluorescence of Dox as well as that of the membrane stain and the nuclear stain. In Figure 4B we show an image of control cells that were pretreated with an excess of trastuzumab to block HER2 binding and then incubated with tmFab-SAv-Bi-MCP-Dox. As in the case of Figure 4A, the Dox emission is mainly localized in the cell cytoplasm, but the overall emission signal from Dox is much weaker than in Figure 4A, reflecting the decreased uptake of tmFab-SAv-Bi-MCP-Dox due to blockage of the HER2 receptors, thus, demonstrating that the binding and internalization of tmFab-SAv-Bi-MCP-Dox was HER2-specific. The MCPs in these experiments were saturated with stable In^{3+}. At pH 7.4, each pendant group with its DTPA-In chelate carries a net charge of −1. These charges along the backbone of the MCP may have an important effect on cell uptake and nuclear localization, as discussed below. In Figure 4C we show results for cells treated with free Dox. Here there is a higher Dox concentration in the cell nucleus, and Dox is also found in the cytoplasm. The high relative intensity of free Dox in the cell nucleus compared to the cytoplasm or cell membrane is consistent with Dox interacting with proteasomes, which enables its transport into the nucleus.[20]

Cell Fractionation Studies. Although the confocal fluorescence images offer qualitative observations about tmFab-SAv-Bi-MCP-Dox internalization into SK-BR-3 cells, more quantitative information could be obtained through cell fractionation experiments using the ^{111}In-labeled complexes. Three RICs were compared: (i) tmFab-SAv-Bi-DTPA without MCPs, (ii) tmFab-SAv-Bi-MCP, and (iii) tmFab-SAv-Bi-MCP-Dox. The results of these cell fractionation experiments are summarized in Figure 5. All three RICs had the greatest

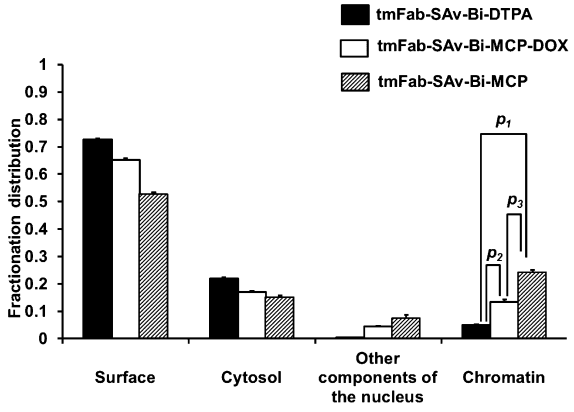

Figure 5. Percentage of RICs radioactivity localized in different cell compartments of SK-BR-3 cells for ^{111}In labeled tmFab-SAv-Bi-DTPA (black column), tmFab-SAv-Bi-MCP-Dox (white column), and tmFab-SAv-Bi-MCP (patterned column). The radioactivity in the nucleus was fractionated into the radioactivity associated with the chromatin and that associated with other components of the nucleus (nuclear membrane, nucleoplasm). Values shown represent the mean ± SEM, n = 3. Significant differences are p_1 = 0.0108, p_2 = 0.00166, and p_3 = 0.0104.

accumulation on the cell membrane. For example, 72.6 ± 0.5% of the total radioactivity for tmFab-SAv-Bi-DTPA was associated with the cell membrane, higher than that of tmFab-SAv-Bi-MCP (52.8 ± 0.5%, p = 0.0056) and tmFab-SAv-Bi-MCP-Dox (65.2 ± 0.7%, p = 0.0012). There were significant differences in the amount of internalized radioactivity. Of the tmFab-SAv-Bi-DTPA bound to the cells, 22 ± 0.3% was present in the cytoplasm, with 5.5 ± 0.3% in the nucleus, almost all of which (i.e., 5.0 ± 0.3%) was associated with the chromatin. tmFab-SAv-Bi-MCP-Dox had an almost equal distribution in the cytoplasm (17.0 ± 0.3%) and in the nucleus (17.8 ± 1.0%) with 13.4 ± 0.9% of the total radioactivity in association with chromatin. The tmFab-SAv complex with the MCP but without the terminal Dox (tmFab-SAv-Bi-MCP) had the highest internalized fraction as well as the highest amount of nuclear localization, with 32.0 ± 0.9% nuclear uptake (24.4 ± 0.6% in the chromatin fraction) and 15.2 ± 0.6% remaining in the cytosol. The values of the distribution percentage for the different RICs are collected in Table S1.

There are several points to highlight based on the data shown in Figure 5. First, although all three RICs exhibit different

dx.doi.org/10.1021/bm401483a | *Biomacromolecules* 2014, 15, 715−725

distribution profiles, they all have the greatest accumulation on the cell surface. It is known that receptor-mediated internalization is normally promoted by bivalent binding. In our case, the use of Fab fragments in the RICs might compromise the internalization ability.[32] Second, the short penetration range of Auger electrons accompanying radioactive decay of ^{111}In means that complexes carrying ^{111}In will be most effective at killing cancer cells when the decay occurs in proximity of the nuclear DNA. Our finding that both MCP-containing complexes are accumulated more efficiently in the cell nucleus and have a strong tendency to associate with the chromatin is an intriguing and promising finding for the application of these polymers to deliver ^{111}In to DNA for Auger electron radiotherapy of cancer. Third, we were surprised to find that the terminal Dox group on tmFab-SAv-Bi-MCP-Dox led to less nuclear localization than the essentially identical polymer (tmFab-SAv-Bi-MCP) without Dox. The protonated amine group on doxorubicin may be necessary for the formation of Dox-proteasome complex and subsequent transport of Dox into the nucleus.[33,34] An alternative polymer with the Dox attached as an alkylamine[22] or through the ketone as a hydrazide might be a more effective strategy for further promoting nuclear localization. From this point of view, it may be the way we attached the terminal Dox group to the polymer that interfered with its ability to transport the complexes to the cell nucleus and the DNA.

Others have reported that trastuzumab, when conjugated to charged macromolecules, undergoes enhanced uptake in SK-BR-3 cells. Miyano et al.[35] modified a G6 lysine dendrimer with glutamate to generate an anionic structure. They subsequently labeled this dendrimer with a fluorescent dye and conjugated it to trastuzumab. These dendrimer-modified trastuzumab showed more rapidly internalization to SK-BR-3 cells than dye-labeled trastuzumab. Chan et al. conjugated trastuzumab with a DTPA-derivatized G4 PAMAM dendrimer and labeled it with ^{111}In. In a cell fractionation study, this antibody–dendrimer conjugate was compared with an identical conjugate modified with an NLS-containing peptide. Both constructs showed similar levels of nuclear uptake. The results showed that the presence of dendrimer promoted cell uptake as well as nuclear importation in SK-BR-3 cells and that conjugation of the NLS peptide did not show any improvement.[36]

The fact that a significant fraction of the tmFab-SAv-Bi-MCP complexes reach the nucleus points to a mechanism that promotes endosomal release. It has been proposed that anionic polymers are responsive to the acidic conditions inside the endosome, and protonation of the polymer leads to morphology changes that subsequently destabilize the endosomal membrane.[37−39] For example, anionic polyelectrolytes have been used to deliver antibody-polymer complexes, oligonucleotides, and other biomolecules into the cell cytoplasm by promoting escape from endosomes.[40−42] It is possible that the polyanionic nature of the MCPs similarly destabilizes endosomes, promotes release of the tmFab-SAv-Bi-MCP complexes into the cytoplasm and enhances the opportunity for accumulation in the cell nucleus.

In order to evaluate the effects of charge on nuclear uptake, we carried out an additional set of experiments with a sample of tmFab-SAv-Bi-MCP that was saturated with stable In^{3+} after being labeled with ^{111}In. We have previously shown that there is no loss of free $^{111}In^{3+}$ ions under these conditions.[14−16] The MCP in tmFab-SAv-Bi-MCP carries approximately 50 DTPA pendant groups. When labeled with $^{111}In^{3+}$, only a small fraction of these groups bind In ions. We can infer from the experiments of Majonis et al.[25] that at pH 7.4 (PBS) the mean charge on each DTPA is between −2 to −3. These carboxylates will be partially protonated at the more acidic pH of endosomes and, especially, lysosomes. When the polymer is saturated with trivalent metal ions, each repeat unit carries a charge of −1 (−4 for the 4 −COO(−) groups of DTPA, balanced by the +3 charge of the In^{3+} ion). Because of the tight binding, this metal chelate is not as susceptible to protonation as the free carboxylate ions of DTPA. Experiments with the In-saturated polymer should indicate whether the charge along the polymer backbone affects cell uptake and nuclear localization.

The results of these experiments are presented in Figure 6. The tmFab-SAv-Bi-MCP complexes containing the indium-

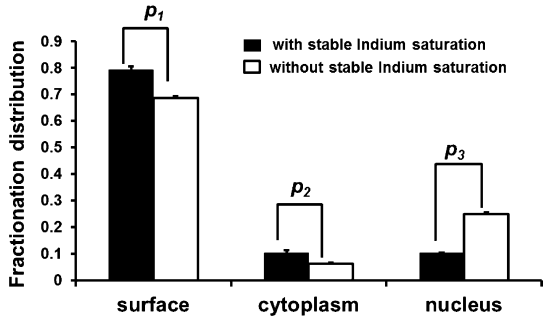

Figure 6. Percentage of radioactivity localized in different cell compartments of SK-BR-3 cells for ^{111}In labeled tmFab-SAv-Bi-MCP with stable indium ion saturation of uncomplexed DTPA groups (black column), tmFab-SAv- Bi-MCP without stable indium ion saturation (white column). Error bars represent the mean ± SEM, n = 3. Significant differences are p_1 = 0.0117, p_2 = 0.0137, p_3 = 0.00514.

saturated polymer have a higher probability of remaining at the surface of SK-BR-3 cells (79.2 ± 1.2%) than those with metal-free DTPA pendant groups (68.7 ± 0.8%; p = 0.0117). Of the fraction taken up by the cells, the fraction of total radioactivity found in the nucleus for the In-saturated polymer (10.3 ± 0.5%) is only about half that of the complexes with metal-free DTPA pendant groups (25.0 ± 0.6%). We conclude that the larger number of negative charges on the polymer not saturated with In^{3+} ions leads to a significant enhancement of nuclear localization compared to the In-saturated polymer complexes, perhaps because of a higher probability of endosomal escape once internalized.

It is interesting that the decrease of negative charges of the polymers due to indium saturation promoted cell membrane retention of tmFab-SAv-Bi-MCP complexes. This might relate to the negative charges on the cell surface, which one anticipates would have a larger repulsive interaction with the MCPs without stable indium saturation than with the MCPs with indium saturation. However, the lower nuclear uptake of the indium saturated MCP-containing complexes suggests that the negative charges elevate their nuclear uptake. This is different from the nuclear uptake mechanism of NLS peptides, which provide positive charges to interact with importins.[43] In summary, the effect of charged polymers in cell internalization is still not well understood. We have much to learn about the effect of polymer charge on interaction with cells and on nuclear localization. The use of MCPs which can be radiolabeled with ^{111}In facilitates quantitative studies to further understand these phenomena.

SUMMARY AND CONCLUSIONS

Through postpolymerization modification of polymers synthesized by RAFT polymerization, we synthesized two well-defined Bi-MCPs, both with a mean degree of polymerization $DP_n \approx 50$ and with a biotin (Bi) at the initiating end. Metal chelation was provided by DTPA pendant groups on every monomer unit. One of the polymers (Bi-MCP-Dox) also carried a doxorubicin at the chain terminus, attached through its amino group as an amide. These polymers were conjugated in a 1:1 molar ratio to streptavidin (tmFab-SAv) covalently linked to a trastuzumab Fab fragment through a PEG_{24} spacer. Radiolabeled complexes were formed by incubating tmFab-SAv-Bi-MCP and tmFab-SAv-Bi-MCP-Dox with ^{111}In. A derivative of DTPA monofunctionalized with biotin (Bi-DTPA) was synthesized for comparison with the MCP complexes linked to tmFab-SAv and labeled with ^{111}In.

SPR measurements for tmFab-SAv, tmFab-SAv-Bi-MCP-Dox, and tmFab-SAv-Bi-MCP revealed that neither the complexation of polymer nor the presence of the terminal Dox significantly affected the binding affinity between the tmFab and ECD of HER2.

Confocal microscopy measurements showed that tmFab-SAv-Bi-MCP-Dox was taken up by SK-BR-3 cells, and a significant fraction of these complexes entered the nucleus. Pretreatment with excess trastuzumab reduced cellular uptake. In parallel, we carried out cell fractionation studies on tmFab-SAv-Bi-MCP-Dox and on tmFab-SAv-Bi-MCP labeled with ^{111}In. Both radiolabeled complexes showed cell internalization and nuclear localization. We conclude that metal-chelating polymers with this composition appear to encourage internalization, nuclear uptake, and chromatin (DNA) binding of trastuzumab fragments modified with streptavidin in human breast cancer cells expressing HER2. Covalent attachment of doxorubicin to the MCPs actually led to a small reduction in cell uptake and nuclear uptake. Further study is needed to understand the impact of polymer charges on cellular uptake and distribution to intracellular compartments.

ASSOCIATED CONTENT

Supporting Information

Additional experimental details, including instrumentation, synthesis of Bi-EO_2NH_2, doxorubicin-maleimide, and of monobiotin-DTPA and Bi-PAAm $(DTPA)_{50}$-disulfide (polymer **4**); ^{1}H NMR spectra of Bi-PBocNAAm-50 (polymer **1**) and Bi-DTPA, HPLC-MS chromatograms of Bi-EO_2NH_2, p-SCN-Bn-DTPA, Bi-DTPA before and after purification; doxorubicin and Dox-maleimide; ESI and MALDI-TOF mass spectra of Dox-maleimide; HPLC chromatograms of Bi-MCP-Dox, tmFab-SAv, and tmFab-SAv-Bi-MCP-Dox; tables with results of cell fractionation studies of tmFab-SAv-Bi-DTPA, tmFab-SAv-Bi-MCP-Dox, and tmFab-SAv-Bi-MCP in SK-BR-3 cells. This material is available free of charge via the Internet at http://pubs.acs.org.

AUTHOR INFORMATION

Corresponding Author

*E-mail: raymond.reilly@utoronto.ca; mwinnik@chem.utoronto.ca.

Notes

The authors declare no competing financial interest.

ACKNOWLEDGMENTS

The authors acknowledge the financial support from the Canadian Institutes of Health Research/Natural Sciences and Engineering Research Council Collaborative Health Research Program (Grant No. CHRPJ 365423-09; CPG-95268) and from DVS Sciences, Inc. We also thank Mr. Serge Zaretsky, who assisted with the HPLC-MS measurements, and Mr. Nick Jarvik for his assistance with the SPR experiments as well as helpful discussions.

REFERENCES

(1) Shepard, H. M.; Lewis, G. D.; Sarup, J. C.; Fendly, B. M.; Maneval, D.; Mordenti, J.; Figari, I.; Kotts, C. E.; Palladino, M. A., Jr.; Ullrich, A. *J. Clin. Immunol.* **1991**, *11*, 117−127.

(2) Kapitanovic, S.; Radosevic, S.; Kapitanovic, M.; Andelinovic, S.; Ferencic, Z.; Tavassoli, M.; Primorac, D.; Sonicki, Z.; Spaventi, S.; Pavelic, K.; et al. *Gastroenterology* **1997**, *112*, 1103−1113.

(3) Maguire, H. C.; Greene, M. I. *Semin. Oncol* **1989**, *16*, 148−155.

(4) Press, M. F.; Pike, M. C.; Hung, G.; Zhou, J. Y.; Ma, Y.; George, J.; Dietz-Band, J.; James, W.; Slamon, D. J.; Batsakis, J. G. *Cancer Res.* **1994**, *54*, 5675−5682.

(5) Slamon, D. J.; Clark, G. M.; Wong, S. G.; Levin, W. J.; Ullrich, A.; McGuire, W. L. *Science* **1987**, *235*, 177−182.

(6) Di Fiore, P. P.; Pierce, J. H.; Kraus, M. H.; Segatto, O.; King, C. R.; Aaronson, S. A. *Science* **1987**, *237*, 178−182.

(7) Hudziak, R. M.; Lewis, G. D.; Holmes, W. E.; Ullrich, A.; Shepard, H. M. *Cell Growth Differ.* **1990**, *1*, 129−134.

(8) (a) Batra, J. K.; Kasprzyk, P. G.; Bird, R. E.; Pastan, I.; King, C. R. *Proc. Natl. Acad. Sci. U.S.A.* **1992**, *89*, 5867−5871. (b) Rosenblum, M. G.; Shawver, L. K.; Marks, J. W.; Brink, J.; Cheung, L.; Langton-Webster, B. *Clin. Cancer Res.* **1999**, *5*, 865−874. (c) Wels, W.; Harwerth, I.-M.; Mueller, M.; Groner, B.; Hynes, N. E. *Cancer Res.* **1992**, *52*, 6310−6317.

(9) Carter, P.; Presta, L.; Gorman, C. M.; Ridgway, J. B.; Henner, D.; Wong, W. L.; Rowland, A. M.; Kotts, C. M. E. C.; Carver, M. E.; Shepard, H. M. *Proc. Natl. Acad. Sci. U.S.A.* **1992**, *89*, 4285−4289.

(10) Nahta, R.; Esteva, F. J. *Cancer Lett.* **2006**, *232*, 123−138.

(11) Rosenblum, M. G.; Horn, S. A.; Cheung, L. H. *Int. J. Cancer* **2000**, *88*, 267−273.

(12) Coyne, C. P.; Ross, M. K.; Bailey, J. G. *J. Drug Targeting* **2009**, *17*, 474−489.

(13) Lambert, J. M. *Curr. Opin. Pharmacol.* **2005**, *5*, 543−549.

(14) Phillips, G. D. L.; Li, G.; Dugger, D. L.; Crocker, L. M.; Parsons, K. L.; Mai, E.; Blättler, W. A.; Lambert, J. M.; Chari, R. V.; Lutz, R. J. *Cancer Res.* **2008**, *68*, 9280−9290.

(15) Costantini, D. L.; Chan, C.; Cai, Z.; Vallis, K. A.; Reilly, R. M. *J. Nucl. Med.* **2007**, *48*, 1357−1368.

(16) Torchilin, V. P. *Bioconjugate Chem.* **1998**, *10*, 146−149.

(17) Boyle, A. J.; Liu, P.; Lu, Y.; Weinrich, D.; Scollard, D. A.; Ngo Njock Mbong, G.; Winnik, M. A.; Reilly, R. M. *Pharm. Res.* **2013**, *30*, 104−16.

(18) Liu, P.; Boyle, A. J.; Lu, Y.; Reilly, R. M.; Winnik, M. A. *Biomacromolecules* **2012**, *13*, 2831−42.

(19) Lu, Y.; Chau, M.; Boyle, A. J.; Liu, P.; Niehoff, A.; Weinrich, D.; Reilly, R. M.; Winnik, M. A. *Biomacromolecules* **2012**, *13*, 1296−1306.

(20) Kiyomiya, K.; Matsuo, S.; Kurebe, M. *Cancer Res.* **2001**, *61*, 2467−2471.

(21) Costantini, D. L.; Villani, D. F.; Vallis, K. A.; Reilly, R. M. *J. Nucl. Med.* **2010**, *51*, 477−483.

(22) Ickenstein, L. M.; Edwards, K.; Sjöberg, S.; Carlsson, J.; Gedda, L. *Nucl. Med. Biol.* **2006**, *33*, 773−783.

(23) Colwill, K.; Gräslund, S. *Nat. Methods* **2011**, *8*, 551−558.

(24) Reilly, R. M.; Kiarash, R.; Cameron, R. G.; Porlier, N.; Sandhu, J.; Hill, R. P.; Vallis, K.; Hendler, A.; Gariépy, J. *J. Nucl. Med.* **2000**, *41*, 429−438.

(25) Majonis, D.; Herrera, I.; Ornatsky, O.; Schulze, M.; Lou, X.; Soleimani, M.; Nitz, M.; Winnik, M. A. *Anal. Chem.* **2010**, *82*, 8961−8969.
(26) Vaneycken, I.; Devoogdt, N.; Van Gassen, N.; Vincke, C.; Xavier, C.; Wernery, U.; Muyldermans, S.; Lahoutte, T.; Caveliers, V. *FASEB J.* **2011**, *25*, 2433−2446.
(27) Troise, F.; Cafaro, V.; Giancola, C.; D'Alessio, G.; De Lorenzo, C. *FEBS J.* **2008**, *275*, 4967−4979.
(28) Bostrom, J.; Haber, L.; Koenig, P.; Kelley, R. F.; Fuh, G. *PloS One* **2011**, *6*, e17887.
(29) Chan, C.; Scollard, D. A.; McLarty, K.; Smith, S.; Reilly, R. M. *EJNMMI Res.* **2011**, *1*, 15.
(30) (a) Bagalkot, V.; Farokhzad, O. C.; Langer, R.; Jon, S. *Angew. Chem., Int. Ed.* **2006**, *45*, 8149−8152. (b) Gillies, E. R.; Fréchet, J. M. J. *Bioconjugate Chem.* **2005**, *16*, 361−368.
(31) Zhu, W.; Okollie, B.; Artemov, D. *Cancer Biol. Ther.* **2007**, *6*, 1960−1966.
(32) Fan, Z.; Lu, Y.; Wu, X.; Mendelsohn, J. *J. Biol. Chem.* **1994**, *269*, 27595−27602.
(33) Minotti, G.; Menna, P.; Salvatorelli, E.; Cairo, G.; Gianni, L. *Pharmacol. Rev.* **2004**, *56*, 185−229.
(34) Kiyomiya, K.; Matsuo, S.; Kurebe, M. *Life Sci.* **1998**, *62*, 1853−1860.
(35) Miyano, T.; Wijagkanalan, W.; Kawakami, S.; Yamashita, F.; Hashida, M. *Mol. Pharmaceutics* **2010**, *7*, 1318−1327.
(36) Chan, C.; Cai, Z.; Reilly, R. *Pharm. Res.* **2013**, *30*, 1999−2009.
(37) Yessine, M.-A.; Leroux, J.-C. *Adv. Drug Delivery Rev.* **2004**, *56*, 999−1021.
(38) Breunig, M.; Bauer, S.; Goepferich, A. *Eur. J. Pharm. Biopharm.* **2008**, *68*, 112−128.
(39) Lackey, C. A.; Murthy, N.; Press, O. W.; Tirrell, D. A.; Hoffman, A. S.; Stayton, P. S. *Bioconjugate Chem.* **1999**, *10*, 401−405.
(40) Bulmus, V.; Woodward, M.; Lin, L.; Murthy, N.; Stayton, P.; Hoffman, A. *J. Controlled Release* **2003**, *93*, 105−120.
(41) Lackey, C. A.; Press, O. W.; Hoffman, A. S.; Stayton, P. S. *Bioconjugate Chem.* **2002**, *13*, 996−1001.
(42) Berguig, G. Y.; Convertine, A. J.; Shi, J.; Palanca-Wessels, M. C.; Duvall, C. L.; Pun, S. H.; Press, O. W.; Stayton, P. S. *Mol. Pharm.* **2012**, *9*, 3506−3514.
(43) Costantini, D. L.; Hu, M.; Reilly, R. M. *Cancer Biother. Radiopharm.* **2008**, *23*, 3−24.